


Liquid and ice water content in clouds and their variability with temperature in Africa based on ERA-Interim, JRA-55, MERRA and ISCCP

Didier Ntwali^{1,2,3}  · Emmy Mugisha⁴ · Floribert Vuguziga³ · Didier Kakpa⁵

Received: 22 June 2015 / Accepted: 15 February 2016
© Springer-Verlag Wien 2016

Abstract This study presents seasonal vertical structure from 1000 to 100 hPa of liquid water content (LWC) and ice water content (IWC) and investigates their variability with temperature in Africa from climatological perspective. Both LWC and IWC may increase or decrease with temperature by season and by region. We compared vertical distribution of LWC and IWC from ERA-Interim, JRA-55 and MERRA reanalysis to the distribution of cloud types from ISCCP and we found that cloud type with highest liquid content is Stratocumulus (Sc) in JJA for both East of Africa (13.3 %) and West of Africa (19.3 %) while Cumulus (Cu) in MAM for both South of Africa (8.6 %) and North of Africa (13.5 %). Cirrus (Ci) is the most frequent cloud with ice with

24.6 % presence in East Africa, 20.4 % in West Africa, 7.2 % in North Africa during MAM and 21.3 % in South Africa during SON. The LWC exists below 400 hPa for both ERA-I and JRA-55, whereas below 200 hPa based on MERRA in all regions of Africa. The IWC exists above 600 hPa for both East and West Africa, above 800 hPa in South Africa and above 900 hPa in North Africa for both ERA-I and JRA-55, whereas above 500 hPa in both East and West of Africa, above 800 hPa in South of Africa and above 850 hPa in North of Africa based on MERRA. The ERA-I, JRA-55 and MERRA are in agreement in low and mid troposphere while in upper troposphere only ERA-I and JRA-55 are in agreement. The MERRA disagrees with ERA-I and JRA-55 in the upper troposphere. The difference of LWC and IWC seasonal vertical distribution in Africa is due to different climatic features between tropic regions and subtropic regions. All three reanalyses show the LWC and IWC between -22.7 and 1.6 °C over Africa. The coexistence temperature between LWC and IWC may be useful to estimate the temperature at which there are the supercooled liquid water and mixed clouds. The ERA-I and JRA-55 may be good proxies in precipitation and cloud monitoring in regions with a lack of in situ observations in Africa. Our results reveal that ISCCP and the two reanalyses (ERA-I and JRA-55) are more reliable for characterizing cloud types and the vertical profile of LWC and IWC climatology, respectively.

Responsible Editor: R. Roebeling.

✉ Didier Ntwali
ntwalididi@yahoo.fr; ntwalididier@mail.iap.ac.cn

Emmy Mugisha
emymugi@gmail.com

Floribert Vuguziga
vfloribert@yahoo.com

Didier Kakpa
kakpad@yahoo.fr

¹ Institute of Atmospheric Physics, Chinese Academy of Sciences (CAS), Beijing, China

² University of Chinese Academy of Sciences (UCAS), Beijing, China

³ Rwanda Meteorology Agency (Meteo Rwanda), P.O. Box 898, Kigali, Rwanda

⁴ Nanjing University of Science and Technology, Nanjing, China

⁵ Direction Nationale de la Météorologie du Bénin, Cotonou, Benin

1 Introduction

Clouds are formed by different physical and dynamical processes that are strongly dependent on liquid water content and ice water content (Gultepe and Isaac 1997).

The term liquid clouds refers to clouds that do not contain ice particles, the term ice clouds is applied to clouds that do not contain water droplets and the term mixed clouds is reserved to clouds where water droplets and ice particles coexist (Mazin 2006). In this study, we analyzed vertical structure of cloud liquid water content and cloud ice content derived by ERA-interim, which is in contrast to former studies where aircrafts (Vidaurre et al. 2011; Boudala et al. 2004) and probes were used to measure liquid water content (Gultepe and Isaac 1997; Vidaurre et al. 2011) and to study the microphysical characterization of mixed-phase clouds (Korolev et al. 2003). Many studies have analyzed precipitation amounts in Africa but there are few studies about the cloud microphysics, which play a big role in precipitation formation. This study analyses how cloud microphysics impacts East of Africa, West of Africa, South of Africa and North of Africa during all seasons. Cloud water and cloud ice are predicted to form through large-scale condensation and deposition processes (Fowler et al. 1996). Previous studies based on satellite observations done by DelGenio and Wolf (2000) showed no liquid water content (LWC) at temperature less than $-10\text{ }^{\circ}\text{C}$, while another study based on the situ observations done by Gultepe et al. (2002) indicated that approximately 40–50 % are at temperatures less than $-10\text{ }^{\circ}\text{C}$. The saturation vapor pressure over liquid water is higher than that over ice at low temperatures, which explains the difference of the growth rate of ice particles and liquid droplets under the same conditions (Korolev and Isaac 2003). The presence of liquid and ice in the same volume is colloiddally unstable, as the liquid will easily be taken up by ice (Harrington et al. 1999). Previous studies indicated that clouds in the temperature range between -30 and $0\text{ }^{\circ}\text{C}$, 30–60 % of are supercooled liquid water while 40–60 % in mixed phase clouds (Zhang et al. 2010; Mazin 2006). The LWC generally increases with the decrease of height for synoptic snow profiles, resulting in the highest LWC values in low portion of the cloud layer, while for shallow middle-level clouds, higher values are near cloud top (Noh et al. 2013). In northern latitudes the cloud liquid water content data were classified at temperature intervals between -30 and $25\text{ }^{\circ}\text{C}$. Gultepe and Isaac (1997) showed that LWC increased from 0.04 g m^{-3} at $-27.5\text{ }^{\circ}\text{C}$ to 0.23 g m^{-3} at $2.5\text{ }^{\circ}\text{C}$ and started to decrease until the temperature reaches $17.5\text{ }^{\circ}\text{C}$, while at the lowest altitude the maximum LWC was 0.26 g m^{-3} at $22.5\text{ }^{\circ}\text{C}$. There were no cloud liquid water content for temperature less than $15\text{ }^{\circ}\text{C}$ in the studies done by Smith (1990) and Moss and Johnson (1994). While considering chemical composition in cloud water, Moller et al. (1996) found that there were sharp decreases or increases of LWC within a time scale between a few minutes and one hour, which showed an ending or beginning of the cloud event. The maximum LWC was detected

in mid-troposphere based on the ERA-interim and in low troposphere based on CloudSat, while both showed the maximum ice water content (IWC) in the upper troposphere (Jiang et al. 2011). There is a difference between vertical distributions of cloud water and cloud ice whereby the maximum of cloud water appears in January in the lower troposphere in the tropics located near the 3-km level and in the equator, whereas the maximum of cloud ice occurs in the tropical upper troposphere (Fowler et al. 1996). Both liquid water path (LWP) and ice water path (IWP) were found to be high over intertropical convergence zone (Yamada and Satoh 2013). The seasonal vertical structure of liquid and ice water content in the troposphere is complex and not well understood despite its regional and global impacts. There is a connection between liquid and ice water content with cloud level type and a significant relationship with temperature by season and by region.

1.1 African climatology

The climate of Africa may be grouped depending on their geography position: in North of Africa the climate is characterized by the significantly low moisture, dry climate, the rainfall amount less than 130 mm/year and the extreme temperature; the West of Africa is a semi-arid region with a steppe climate and the average rainfall per year is between 100 and 200 mm from June through September; the Savanna climate is found in both West and South of Africa characterized by wet and dry seasons during summer and winter, respectively, with rainfall average of 100–400 mm/year; the equatorial region in Africa is a rain-forest (tropical wet) which has wet and warm climate with high amount of rainfall though all year with annual average of 1800 mm (Adeyewa and Nakamura 2003). In Central of Africa there is bimodal structure per year with high maxima in November and March to May (Nikulin et al. 2012). There is high spatial and temporal rainfall amount variability in East Africa (Ogallo 1989) due to the presence of high mountains, the large lakes such as Lake Victoria, the Indian Ocean in the east and the seasonal migration of the intertropical convergence zone (ITCZ) (Ntale et al. 2003). There are two major phenomena which significantly contribute to the local weather and climate over Africa. There are monsoons which are the driving mechanism of the climate and the dust storms from the dry areas which have a profound impact on the weather conditions over Africa; considering the large amount of aerosols, they may have influence on the African monsoon (De Graaf et al. 2009). Africa regions have different rainfall seasons. In many regions of Africa the heavy rainfall most likely occurs in the afternoon and evening (Geerts and Dejene 2005). The inter-

tropical convergence zone (ITCZ) passes across East of Africa twice a year and has significant influence on the climatological rainfall pattern (Anyah and Semazzi 2007). The inter-annual variability in East of Africa is influenced by the El Niño-Southern Oscillation (ENSO) anomaly patterns (Ogallo 1989). North and South Africa are located in midlatitudes, whereas East and West of Africa in tropical regions where the Intertropical Convergence Zone (ITCZ) crosses two times per year. The location of the ITCZ corresponds to the maximum precipitation in rainfall seasons (Nikulin et al. 2012). The regions with high amount of precipitation are located where the ITCZ crosses include tropical regions of Africa (Huffman et al. 1997; Rui and Yunfei 2005). In Africa the ITCZ crosses twice per year in the regions located in the tropics such as East and West of Africa which explain more precipitation in those regions, while regions located in midlatitude such as North and South of Africa don't have more precipitation compared to East and West of Africa due to the fact that the ITCZ reaches in those regions once per year. The rainfall in the tropical regions is a cumulus regime (Riehl 1979), whereas in the midlatitude regions there is large presence of stratiform precipitation in convection-generated clouds (Rutledge and Houze 1987). There are precipitating clouds, entirely convection-generated cumulonimbus in the tropic regions (Houze 1997), which results in large amount of precipitation across East of Africa (Nikulin et al. 2012). In the North of Africa the climate is uniformly dry during JJA and the moisture is almost totally absent in some places except where a few oases exist, while climate with low precipitation with high peaks prevails from June through September (Adeyewa and Nakamura 2003). The rainfall in East of Africa is sensitive to both Atlantic in the west and Indian Ocean in the east (Tierney et al. 2011) and it is influenced by El Niño events, which tend to increase rainfall in some regions and produce drought in other regions (Mike 2002). There are long and short (moist) rainfall seasons in March–April–May and September–October–November (SON), dry season in June–July–August (JJA) and December–January–February (DJF) (Ntale et al. 2003). The strong Congo air mass flowing into the region may increase the instabilities of the convergence zone which leads to the increase of long rains (Okoola 1999). There is significant evidence in the intraseasonal variability in the convective activity and low-level atmospheric circulation during summer monsoon in West of Africa (Janicot and Sultan 2001). In West of Africa during JJA there are convection and moisture advection (Kiladis and Weickmann 1997), which leads to the rainfall. The increase (decrease) of the West African monsoon is associated with a strong cyclonic (anticyclonic) activity over the Sahel which leads to stronger (weaker) moisture

advection in West of Africa (Janicot and Sultan 2001). In West of Africa during the West African Monsoon (WAM) there is maximum rainfall at the end of May/beginning of June and its seasonal variation migration (Nikulin et al. 2012). The austral summer, autumn, winter and spring occur during December to February (DJF), March to May (MAM), June to August (JJA) and September to November (SON), respectively, in South of Africa where the maximum rainfall occurs in DJF (Engelbrecht and Landman 2015). The rainfall which is below the normal amount is due to the El Niño Events (Tozuka et al. 2014). In East of Africa there are high mountains compared to other regions of Africa. The mountains may have effects on the formation of some cloud types. The air moving at the slope of the mountain is transported by the wind. The wind velocity intensity may differ by region and by season. The stratus clouds form in the free atmosphere in rising air currents of only a few cm/s vertical velocity along a very sloping plane (Aufm 1950). In many regions the rainfall increases with elevation due to the orographic updraft (Weisse and Bois 2001). The wind is an important meteorological parameter which influences the distribution of rain in mountainous regions (Moreno et al. 2014).

1.2 Role of aerosols in the variation of cloud properties

There are significant amount of aerosols from deserts and biomass burning in the African continent which may influence the African monsoon (De Graaf et al. 2009). They influence the cloud formation and cloud albedo (Twomey 1977), cloud lifetime (Albrecht 1989), cloud height (Pincus and Baker 1994) and precipitation. There is a strong relationship between the aerosols and the amount of precipitation in Africa (De Graaf et al. 2009) and the cloud coverage may increase or decrease due to aerosol pollution (Ackerman et al. 2000). The smoke from biomass burning and anthropogenic air pollution are known as sources of large concentrations of small cloud condensation nuclei (CCN) (Rosenfeld et al. 2001), which lead to the formation of a high concentration of small cloud droplets and therefore to an increased cloud albedo (Twomey et al. 1987) and also to the suppressed precipitation (Rosenfeld 2000). In June or July the InterTropical Convergence Zone (ITCZ) reaches the north position when there is high dust production in the west of the Sahara desert (De Graaf et al. 2009). The anthropogenic and dust aerosols have different impacts on precipitation amount. When the ITCZ reaches the Sahel region, the general circulation model revealed the reduction and increase of precipitation in the north and south sides of ITCZ respectively (Yoshioka et al. 2007). The suppression of precipitation and change of ice cloud amounts by

mineral aerosols have been detected in North of Africa (Mahowald and Kiehl 2003). We found both the positive and negative correlation between different cloud types and precipitation in the West and East of Africa while only positive correlation in South of Africa (Ntwali 2015). In west of Africa the cumulus (Cu) with liquid and the cirrus (Ci) show negative correlation, whereas stratocumulus (Sc), stratus (St), nimbostratus (Ns), altocumulus (Ac), altostratus (As) and cirrostratus (Cs) show a positive correlation. In East of Africa there are only middle clouds stratus (St) and nimbostratus (Ns) with liquid which show negative correlation, whereas cumulus (Cu), stratocumulus (Sc), altocumulus (Ac), altostratus (As), cirrostratus (Cs) and cirrus (Ci) show a positive correlation. There is a positive correlation between dust and cloud amount whereas there is low negative correlations between high ice clouds (cirrus, stratocirrus and deep convective) and high dust months in North of Africa (Mahowald and Kiehl 2003). In June to October there is a significant biomass burning in South of Africa (Cooke et al. 1996). Their aerosol radiative effects are significantly altered by the inclusion of semidirect effects which are primarily driven by cloud cover and changes in liquid water path over land (Sakaeda et al. 2011). In West of Africa the reduction of precipitation over the Sahel region in West of Africa is the main effect of dust radiative forcing (Fabien et al. 2008; Rosenfeld et al. 2001). Central-east of Africa experiences low (high) aerosol loading during wet (dry) seasons while Southeast Africa shows alternating high and low residues with high values during the local dry season (De Graaf et al. 2009) which are absent during the local wet season (e.g. Stein et al. 2003). The reanalysis data products allow us to make and improve the quality assessments and quantifying uncertainties (Rienecker et al. 2011). This may also explain different LWC and IWC amounts in the same cloud type in Africa. After the Mount Pinatubo eruption, the ISCCP indicated a decrease in Cirrus cloud amount accompanied by an increase of Cumulus and Altocumulus clouds which cause misidentification of Cirrus as low Cumulus clouds (Luo et al. 2002). The significant difference between ERA-Interim and GPCP revealed high uncertainties which may be caused by the underestimation of aerosol optical depth in the region (Dee et al. 2011). The purpose of this study was to reanalyze and evaluate extensively the seasonal vertical profile of LWC and IWC based on ERA-I, JRA-55 and MERRA reanalysis from 1979 to 2014 from climatological perspective and investigate the cloud type with low- and high liquid/ice content based on ISCCP observations in East, West, South and North of Africa. The main goal to use three reanalysis datasets was to clarify their quality and differences over East, West, South and North of Africa by season.

2 Data and methodology

2.1 ERA-Interim reanalysis

The ERA-interim dataset is latest global atmospheric reanalysis produced by the European Centre for Medium-Range Weather Forecasts (ECWMF) to replace ERA-40 and it is continuously updated and extends from 1 January 1979 to present (Dee et al. 2011). The ERA-interim uses data assimilation which improves radiative transfer model (Lindsay et al. 2014). The version of 4D-Var used for ERA-Interim helps the bias corrections needed for the majority of satellite-based radiance observations and to produce accurate analyses of the large-scale tropospheric circulation which involves computing a variational analysis of the basic upper-air atmospheric fields (temperature, wind, humidity, ozone, surface pressure), followed by separate analyses of near-surface parameters (2 m temperature and 2 m humidity), soil moisture, soil temperature, snow and ocean waves (Dee et al. 2011). The cloud liquid water content (LWC), cloud ice water content (IWC) and temperature derived by ERA-interim (ERA-I) reanalysis are used in this study from 1979 to 2014 with 0.75 horizontal resolution and 27 vertical pressure levels (from 1000 to 100 hPa).

2.2 JRA-55 reanalysis

The JRA-55 reanalysis is produced and implemented by Japanese Meteorological Agency (JMA) and uses observations from ERA-40 (Uppala et al. 2005) and the archived data of JMA (Kobayashi et al. 2015). JRA-55 uses the Japanese Meteorological Administration (JMA) global operational forecast model with finer spatial resolution (Yokoi 2015). JRA-55 provides both long period data and using four-dimensional variational method. Even though there are several reanalysis data with long period data, most of them use three dimensional variational analysis method.

2.3 MERRA reanalysis

The Modern-Era Retrospective Analysis for Research and Applications (MERRA) reanalysis dataset was released by NASA in 2010 based on the Goddard Earth Observing System Data Assimilation System Version 5 (GEOS-5) (Rienecker et al. 2011). It provides global reanalysis data products from 1979 to present (Kennedy et al. 2011). The major role of data assimilation in the model is to simulate the hydrological cycle with high accuracy (Lindsay et al. 2014). MERRA was implemented due to the fact that hydrologic cycle represented in previous reanalyses was not sufficient for climate and weather studies (Rienecker et al. 2011). MERRA uses a three-

dimensional variational data assimilation (3DVAR) analysis algorithm based on the Gridpoint Statistical Interpolation scheme (Wu et al. 2002). It uses a GEOS-5 atmospheric general circulation model (AGCM) which is effective for transport in the stratosphere (Pawson et al. 2007). MERRA has 72 vertical levels from the surface to 0.01 hPa (Rienecker et al. 2011) and uses a three-dimensional variational data assimilation (3DVAR) analysis algorithm based on the Gridpoint Statistical Interpolation scheme (Wu et al. 2002) with a 6-h update cycle. NCEP-NCAR reanalysis has been used to implement the MERRA reanalysis due to its latest data.

2.4 ISCCP observations

The ISCCP (International Satellite Cloud Climatology Project) combines visible and infrared to detect clouds and geosynchronous satellites as the preferred satellite source except at high latitudes. The ISCCP data have an archive of more than 20 years of monthly global observations. We used ISCCP due to its capacity to provide long period global cloud data (in this study we used data from 1983 to 2009) and due to the fact that it has shown a close agreement over land with other satellites (SOBS, METEOR and Nimbus). In polar regions, it shows the exception whereby the cloud amounts appear to be too low over land by about 10 % (somewhat less in summer and somewhat more in winter) as well as slightly low over the oceans. The ISCCP has shown that the global annual mean cloud amount is about 63 %, while 23 % higher over oceans than over land and slightly more in nighttime than daytime over oceans, whereas more in daytime than in nighttime cloud amount over land (Rossow et al. 1993). The ISCCP cloud type levels and classification are defined as low cloud pressure level less than 680 hPa, middle cloud level between 680 and 440 hPa and high cloud level above 440 hPa as shown by Rossow and Schiffer (1991). In this study the low-level cloud types analyzed are Stratus (St), Cumulus (Cu) and Stratocumulus (Sc); in middle-level cloud types there are Altostratus (As), Altostratus (As) and Nimbostratus (Ns) and in high cloud types there are Cirrus (Ci) and Cirrostratus (Cs). The ISCCP data are used in this study to evaluate liquid and ice water cloud content variability in the mentioned different types of clouds and to investigate cloud type by seasonal in tropospheric vertical distribution from 1000 hPa to 100 hPa in Africa.

3 Results and discussion

We have considered four regions in Africa shown in Fig. 1 depending on the African geography: East of Africa (28° E to 43° E and -3° S to 5° N), West of Africa (-12° W to

10° E, 3° N to 20° N), South of Africa (17° E to 36° E and -38° S to -5° S) and North of Africa (1° E to 34° E and 20° N to 34° N). The four regions are considered due to their differences in climate variability. In this study we used the seasonal mean of LWC, IWC and temperature for analysis. The seasonal vertical structures of tropospheric LWC and IWC from 1000 to 100 hPa are not the same over East, West, South and North of Africa. The LWC amount changes significantly by region while there is less difference in IWC. The ERA-I and JRA-55 show no LWC above 300 hPa while MERRA above 200 hPa in East of Africa (Fig. 2a–d), West of Africa (Fig. 2e–h), South of Africa (Fig. 2i–l) and North of Africa (Fig. 2m–p). Boucher et al. (1995) found that the increase of cloud coverage is mostly the consequence of increased cloud amount fraction in the lower layers (1000–800 hPa). It is clear that the highest LWC occurs during rainfall season: in West of Africa during JJA (23.4 g m⁻³ at 825 hPa, 21.4 g m⁻³ at 900 hPa, 11.8 g m⁻³ at 500 hPa), in South of Africa during DJF (14.8 g m⁻³ at 825 hPa, 10.9 g m⁻³ at 800 hPa, 14.9 g m⁻³ at 900 hPa) based on ERA-I, JRA-55 and MERRA, respectively (Table 1). In North of Africa the ERA-I and MERRA show highest LWC in DJF rainfall season: 2.9 g m⁻³ at 800 hPa and 3 g m⁻³ at 1000 hPa, respectively, while JRA-55 shows it in SON season (3.7 g m⁻³ at 900 hPa) but no significant difference in DJF rainfall season (3.5 g m⁻³ at 900 hPa). In East of Africa both JRA-55 and MERRA show high LWC during two different rainfall seasons: MAM (12.5 g m⁻³ at 800 hPa) and SON (13 g m⁻³ at 600 hPa), respectively, while the ERA-I shows it in JJA dry season (16.8 g m⁻³ at 650 hPa) but also with high amount in rainfall season (15.270 g m⁻³ at 600 hPa in

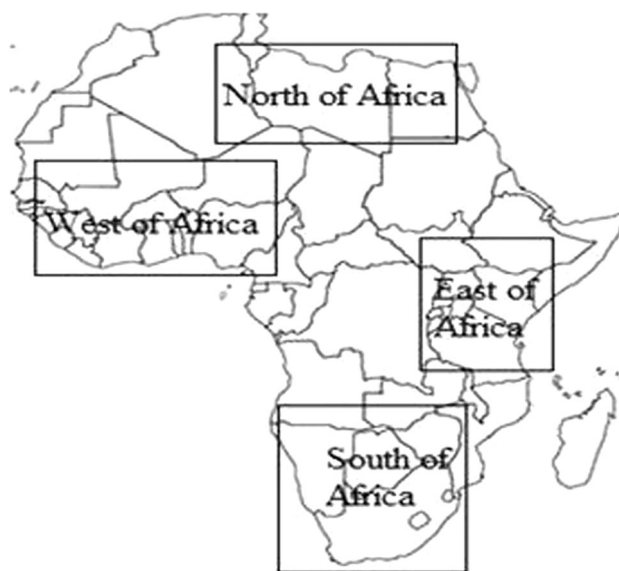


Fig. 1 African map showing East of Africa, West of Africa, South of Africa and North of Africa regions

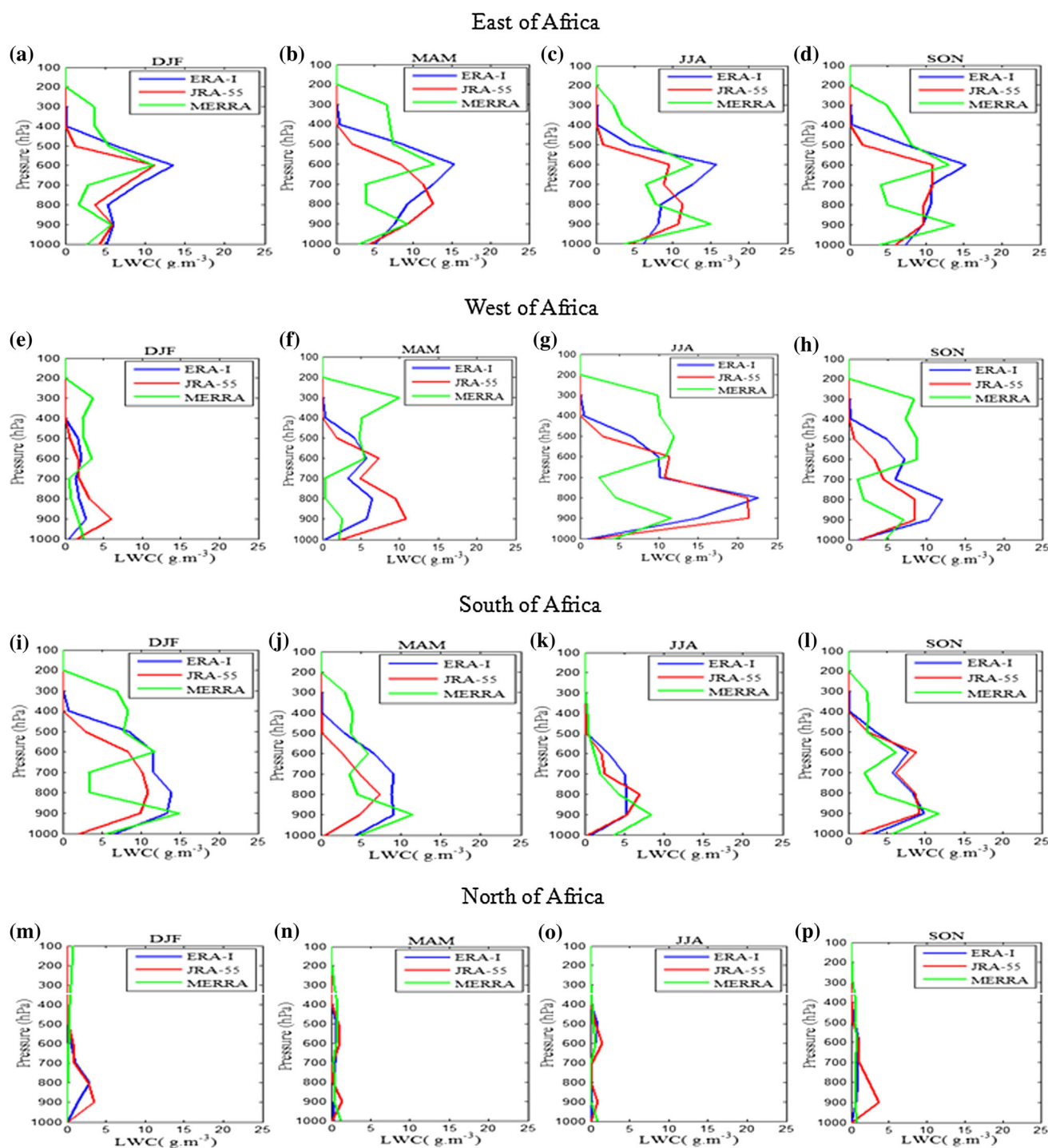


Fig. 2 The seasonal vertical profile of LWC (Liquid water content) (g m^{-3}) in East of Africa during **a** DJF, **b** MAM, **c** JJA, **d** SON; in West of Africa during **e** DJF, **f** MAM, **g** JJA, **h** SON; in South of

Africa during **i** DJF, **j** MAM, **k** JJA, **l** SON and in North of Africa during **m** DJF, **n** MAM, **o** JJA, **p** SON from ERA-I (blue line), JRA-55 (red line) and MERRA (green line) reanalysis from 1979 to 2014

MAM and 15.279 g m^{-3} at 600 hPa in SON). This shows that the sensitivity of LWC and IWC amounts in JJA dry season in East of Africa by ERA-I need to be improved. The LWC amount is relating to the amount of rainfall which explains high values during rainfall seasons. The

LWC vertical distribution is explained by deep convection of low tropospheric clouds. The liquid cloud water in JJA and DJF was found to be in low and middle pressure levels (Gregory and Morris 1996). Cloud particle concentrations and their droplet size distributions vary horizontally and

Table 1 The seasonal average vertical maximum of LWC based on ERA interim, JRA55 and MERRA reanalysis

Max LWC	East of Africa	West of Africa	South of Africa	North of Africa
DJF				
ERA	13.5 g m ⁻³ at 600 hPa	2.9 g m ⁻³ at 875 hPa	14.8 g m ⁻³ at 825 hPa	2.9 g m ⁻³ at 800 hPa
JRA55	11.1 g m ⁻³ at 600 hPa	5.9 g m ⁻³ at 900 hPa	10.9 g m ⁻³ at 800 hPa	3.5 g m ⁻³ at 900 hPa
MERRA	10.9 g m ⁻³ at 600 hPa	3.5 g m ⁻³ at 600 hPa	14.9 g m ⁻³ at 900 hPa	3 g m ⁻³ at 1000 hPa
MAM				
ERA	15.270 g m ⁻³ at 600 hPa	7.4 g m ⁻³ at 825 hPa	9.7 g m ⁻³ at 850 hPa	0.8 g m ⁻³ at 550 hPa
JRA55	12.5 g m ⁻³ at 800 hPa	10.8 g m ⁻³ at 900 hPa	7.3 g m ⁻³ at 800 hPa	1.4 g m ⁻³ at 900 hPa
MERRA	12.652 g m ⁻³ at 600 hPa	5.5 g m ⁻³ at 600 hPa	11.4 g m ⁻³ at 900 hPa	1.2 g m ⁻³ at 1000 hPa
JJA				
ERA	16.8 g m ⁻³ at 650 hPa	23.4 g m ⁻³ at 825 hPa	6.1 g m ⁻³ at 850 hPa	1.1 g m ⁻³ at 550 hPa
JRA55	11.3 g m ⁻³ at 800 hPa	21.4 g m ⁻³ at 900 hPa	6.9 g m ⁻³ at 800 hPa	1.5 g m ⁻³ at 600 hPa
MERRA	12.655 g m ⁻³ at 600 hPa	11.8 g m ⁻³ at 500 hPa	8.4 g m ⁻³ at 900 hPa	0.9 g m ⁻³ at 1000 hPa
SON				
ERA	15.279 g m ⁻³ at 600 hPa	13.5 g m ⁻³ at 825 hPa	10.4 g m ⁻³ at 875 hPa	1.1 g m ⁻³ at 550 hPa
JRA55	11 g m ⁻³ at 600 hPa	8.6 g m ⁻³ at 900 hPa	9.2 g m ⁻³ at 900 hPa	3.7 g m ⁻³ at 900 hPa
MERRA	13 g m ⁻³ at 600 hPa	8.8 g m ⁻³ at 600 hPa	11.7 g m ⁻³ at 900 hPa	0.7 g m ⁻³ at 1000 hPa

vertically (Mazin 2006). The temperature may be below 0 °C and water droplets can still exist in clouds as supercooled droplets. As a matter of fact, cloud temperatures frequently need to get below -10 °C for any significant number of ice particles to form. If a cold cloud contains both ice particles and supercooled droplets, it is a mixed cloud. The LWC vertical profile based on ERA-I, JRA-55 and MERRA profile in East of Africa (Fig. 2a–d), West of Africa (Fig. 2e–h) and South of Africa (Fig. 2i–l) are significantly high than that in North of Africa (Fig. 2m–p) which has low LWC mainly due to the presence of Sahara desert which reduces evaporation. The low LWC amount is found over the major desert regions (Fowler et al. 1996). There is an agreement of ERA-I, JRA-55 and MERRA dataset especially at low-pressure levels in all Africa. There is a remarkable disagreement between MERRA with ERA-I and JRA-55 in all Africa, especially at high-pressure levels, while in South of Africa during DJF (Fig. 2j), West of Africa in JJA (Fig. 2g) and SON (Fig. 2h) and East of Africa in MAM (Fig. 2b), in JJA (Fig. 2c), in SON (Fig. 2d) at middle-pressure levels where it shows a large lapse rate. At high and middle-pressure levels the MERRA has high and low LWC, respectively, than ERA-I and JRA-55 in all Africa. The ERA-I and JRA-55 show high LWC at middle and low-pressure levels in East of Africa (Fig. 2a–d) and North of Africa (Fig. 2m–p), respectively. The liquid water occurs often in low- and middle-level clouds. The ERA-I and JRA-55 show the LWC in both low- and middle-level clouds whereas MERRA shows it from low to up level clouds in all Africa. This shows the limitations of

using MERRA in upper level clouds as no liquid water can be found at high negative temperature due to the conversion of liquid to ice. Both East and West of Africa are located in the tropic regions and are close to the equator where there are often convective clouds, which explains the presence of high LWC compared to South and North of Africa located in midlatitude regions. In the Sahel region in West of Africa the storms are marked by high echo tops and high hydrometeor loading aloft (Geerts and Dejene 2005). The high LWC amount is often abundant in the tropics than in the midlatitudes (Fowler et al. 1996) and occurs in deep convective clouds (Politovich 2003) which often occur in equatorial regions. The rainfall season in West, South and North of Africa occurs during JJA, DJF and DJF, respectively, while in MAM and SON in East of Africa. The increase of LWC in the lower troposphere is in accord with the increase of moisture in the region. It is only in East of Africa that ERA-I, JRA-55 and MERRA show the maximum LWC in different seasons. The JRA-55 and MERRA show the maximum LWC during MAM and SON while the ERA-I shows the maximum LWC in dry season (JJA). Even though ERA-I shows the maximum LWC in dry season (16.8 g m⁻³ at 650 hPa in JJA), it shows also high LWC in rainfall seasons (15.270 g m⁻³ at 600 hPa in MAM and 15.279 g m⁻³ at 600 hPa in SON). Cumuliform clouds tend to have large drops which explains the high LWC amount at the low- and mid-pressure levels in which Cumulus and Stratocumulus clouds often occur in high amounts in all Africa. The annual Cumulus and Stratocumulus cloud amounts with liquid are 8.6, 7.9, 7.4, 10.3 %

and 9.7, 12.6, 6.8, 9.2 % in East, West, South and North of Africa, respectively (Fig. 5). The LWC generally increases with altitude and varies from cloud to cloud and also within the same cloud (Politovich 2003). There is an increase of LWC in the low troposphere with the presence of dust whereas there is a decrease of LWC in the middle troposphere with no dust effects, and the reduction of cloud thickness is consistent with the decrease of precipitation (Fabien et al. 2008). Both East and West of Africa are located in the tropics regions and are close to the equator where there are often convective clouds which explain the presence of high LWC compared to South and North of Africa located in midlatitude regions. The high LWC amount is often abundant in the tropics than in the mid-latitudes (Fowler et al. 1996) and occurs in deep convective clouds (Politovich 2003) which often occur in equatorial regions. The increase of LWC in the lower troposphere is in accord with the increase of moisture in the region. It is only in East Africa that ERA-I, JRA-55 and MERRA show the maximum LWC in different seasons. Cumuliform clouds tends to have large drops which explains the high LWC amount at the low- and mid-pressure levels in which Cumulus and Stratocumulus clouds often occur in high amounts in all Africa. The maximum LWC mostly exists at 600 hPa for ERA-I, JRA55 and MERRA in East of Africa while in West, South and North of Africa it exists at different pressure levels (Table 1). When a cloud extends to altitudes where the temperature is colder than 0 °C, ice crystals may form. Cold clouds can consist of supercooled droplets or ice particles or a mixture of both. The probability of ice particles being present in a cold cloud increases as the temperature decreases below 0 °C. The growth of ice crystals may occur due to the direct deposition of vapor to the solid phase, drops colliding with and freezing on the ice particles and ice crystals that grow by collision with other crystals. The droplets' size freezes spontaneously at different temperature. In this study we did not analyze the cloud droplet size as no reanalysis dataset provides vertical profile data of cloud droplet size. There is an agreement of ERA-I, JRA-55 and MERRA of IWC seasonal vertical profile in Africa, especially at low- and middle-pressure levels (Fig. 3). MERRA shows high IWC than ERA-I and JRA-55 at high-pressure levels in all Africa with a large lapse rate in East and West of Africa in all seasons. JRA-55 has low IWC in all seasons at high-pressure levels in all Africa than ERA-I and MERRA. At middle-pressure levels in all seasons MERRA has low IWC than ERA-I and JRA-55 in all Africa. In all seasons the ERA-I has IWC between that of JRA-55 and MERRA in all Africa. In both East of Africa (Fig. 3a–d) and West of Africa (Fig. 3e–h), the JRA-55 shows the IWC in clouds from 600 hPa in all seasons. The East and West of Africa regions located in the tropics have high IWC amount

compared to the North and South of Africa regions located in midlatitude regions. The IWC vertical distribution IWC is explained by deep convection for upper tropospheric clouds. The maximum IWC is found in the middle troposphere for both ERA-I and JRA-55, whereas in the upper troposphere for MERRA. It was shown that the zonal wind RMS error for ERA-I, JRA-55, CFSR and MERRA reanalysis increases with height, especially at upper levels, whereby the differences among them are significant at 200 hPa, with the smallest error in JRA-55 and the largest error in MERRA, while ERA-I shows also small error in mid-to upper troposphere (Chen et al. 2014). The RMS error of temperature remains stable or increases slowly at middle levels while it increases relatively fast at upper levels (Chen et al. 2014). On the average, ERA-I produces mean values consistent with the verifying soundings for temperature and has small RMS error (Bao and Zhang 2013). The RMS error of relative humidity of three reanalyses increases with height, where it is smaller in JRA-55 and ERA-I than in MERRA (Chen et al. 2014). The dust has the influence on the increase of precipitation which is related to the convection as indicated by reduced outgoing longwave radiation (Gu et al. 2012). MERRA shows extreme large intensities than other reanalyses (ERA-Interim, JRA-25 and CFSR), followed by CFSR and then ERA-Interim, and the weakest extremes are found in JRA-25 (Hodges et al. 2011). The mean amplitude of low-level wind at 850 hPa of ERA-I, JRA-55 and MERRA was found to be 0.7, 1.0 and 1.7 m s⁻¹, respectively, while at upper levels the ERA-I has low vertical extent and MERRA shows large diurnal amplitude at upper levels (Chen et al. 2014). For the 925-hPa winds, JRA-25 consistently shows the weakest extreme winds compared with the other reanalyses, although it appears more similar to ERA-Interim than with other reanalyses (Hodges et al. 2011). At upper levels, a northerly wind is seen in ERA-Interim, JRA-55 and MERRA, while with a relatively large diurnal amplitude in MERRA (Chen et al. 2014). The maximum LWCs and IWCs in all Africa are not found at the same pressure level (Tables 1, 2). Both ERA-I and MERRA show the large average vertical LWC amount in East of Africa (15.175 and 12.27 g m⁻³, respectively) while JRA-55 shows it in West of Africa (11.67 g m⁻³). The highest amount of LWC is in East Africa may be explained by many convective systems which occur in that region, especially those which are close to the equator. These results are in agreement with ISCCP which shows high annual average amount of Stratocumulus in East of Africa (9.7 %) and in West of Africa (12.6 %) (Fig. 5). The presence of high amounts of Stratocumulus as cloud with liquid content in East and West of Africa explains the reason of having high LWC in East and West of Africa. The low average vertical LWC amount is shown in North

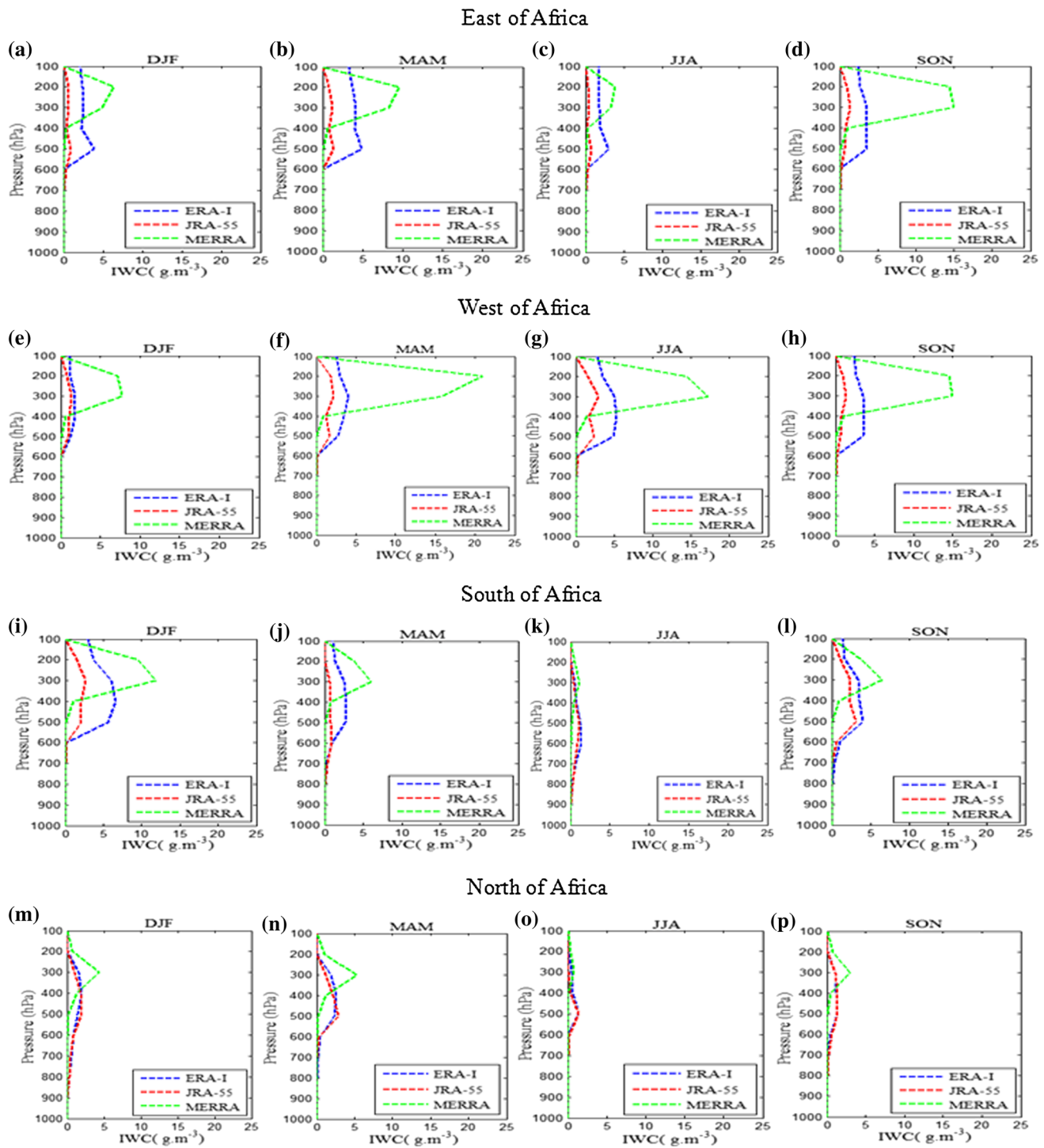


Fig. 3 The seasonal vertical profile of IWC (Liquid water content) (g m^{-3}) in East of Africa during **a** DJF, **b** MAM, **c** JJA, **d** SON; in West of Africa during **e** DJF, **f** MAM, **g** JJA, **h** SON; in South of Africa during **i** DJF, **j** MAM, **k** JJA, **l** SON and in North of Africa during **m** DJF, **n** MAM, **o** JJA, **p** SON from ERA-I (blue line), JRA-55 (red line) and MERRA (green line) reanalysis from 1979 to 2014

of Africa by all three reanalyses: 1.475, 2.52, 1.45 g m^{-3} based on ERA-I, JRA-55 and MERRA, respectively. There is some differences between the detection of low cloud content and the low amount of Stratocumulus (Sc) detected

by ISCCP (6.8 % in South of Africa whereas 9.2 % in North of Africa) (Fig. 5). The ISCCP is in agreement with the ISCCP which shows low amount of Stratocumulus in North of Africa (9.2 %). The Stratocumulus amount is too

Table 2 The seasonal average vertical maximum of IWC based on ERA interim, JRA55 and MERRA reanalysis

Max IWC	East of Africa	West of Africa	South of Africa	North of Africa
DJF				
ERA	3.9 g m ⁻³ at 500 hpa	1.8 g m ⁻³ at 300 hpa	6.8 g m ⁻³ at 350 hpa	1.9 g m ⁻³ at 400 hpa
JRA55	0.9 g m ⁻³ at 500 hpa	1.3 g m ⁻³ at 300 hpa	2.6 g m ⁻³ at 300 hpa	1.9 g m ⁻³ at 500 hpa
MERRA	6.3 g m ⁻³ at 200 hpa	7.6 g m ⁻³ at 300 hpa	11.8 g m ⁻³ at 300 hpa	4.3 g m ⁻³ at 300 hpa
MAM				
ERA	4.9 g m ⁻³ at 500 hpa	4 g m ⁻³ at 300 hpa	2.8 g m ⁻³ at 350 hpa	2.8 g m ⁻³ at 450 hpa
JRA55	1.3 g m ⁻³ at 500 hpa	2.2 g m ⁻³ at 300 hpa	0.9 g m ⁻³ at 600 hpa	2.9 g m ⁻³ at 500 hpa
MERRA	9.5 g m ⁻³ at 200 hpa	20.8 g m ⁻³ at 200 hpa	6 g m ⁻³ at 300 hpa	5.2 g m ⁻³ at 300 hpa
JJA				
ERA	3 g m ⁻³ at 500 hpa	5.3 g m ⁻³ at 400 hpa	1.3 g m ⁻³ at 600 hpa	1.3 g m ⁻³ at 500 hpa
JRA55	0.8 g m ⁻³ at 500 hpa	2.9 g m ⁻³ at 300 hpa	1.1 g m ⁻³ at 500 hpa	1.3 g m ⁻³ at 500 hpa
MERRA	3.9 g m ⁻³ at 200 hpa	17.2 g m ⁻³ at 300 hpa	1.1 g m ⁻³ at 300 hpa	0.7 g m ⁻³ at 300 hpa
SON				
ERA	4.9 g m ⁻³ at 500 hpa	3.6 g m ⁻³ at 350 hpa	4.1 g m ⁻³ at 500 hpa	1.3 g m ⁻³ at 500 hpa
JRA55	1.2 g m ⁻³ at 500 hpa	1.4 g m ⁻³ at 300 hpa	3.1 g m ⁻³ at 500 hpa	1.3 g m ⁻³ at 400 hpa
MERRA	6.3 g m ⁻³ at 300 hpa	14.9 g m ⁻³ at 300 hpa	6.5 g m ⁻³ at 300 hpa	3 g m ⁻³ at 300 hpa

large compared to other low and middle cloud except the Altostratus (As) which may have liquid water, which is the main reason that we compare it with the reanalysis results. The Altostratus (As) shows also high values in North of Africa (8.5 %) and East of Africa (7.7 %) (Fig. 5). The Table 2 shows the seasonal average vertical maximum of IWC based on ERA-I, JRA-55 and MERRA. In East of Africa the ERA-I and JRA-55 show high IWC amount in middle troposphere during MAM rainfall (4.95 g m⁻³ at 500 hPa, 1.3 g m⁻³ at 500 hPa, respectively) while MERRA shows it in the upper troposphere in MAM rainfall season (9.5 g m⁻³ at 200 hPa). In West of Africa the ERA-I and JRA-55 show high IWC amounts in the upper troposphere during JJA rainfall season (5.3 g m⁻³ at 400 hPa and 2.9 g m⁻³ at 300 hPa, respectively) while MERRA shows it also in the upper troposphere but during MAM dry season (20.8 g m⁻³ at 200 hPa). In South of Africa the ERA-I and MERRA show high IWC amount in the upper troposphere during DJF rainfall season (6.8 g m⁻³ at 350 hPa and 11.8 g m⁻³ at 300 hPa, respectively) while JRA-55 shows it in SON season (3.1 g m⁻³ at 500 hPa). It is only in North of Africa that the maximum IWC does not occur in DJF rainfall season, whereby all three reanalyses show it during MAM: at the middle troposphere (2.8 g m⁻³ at 450 hPa and 2.9 g m⁻³ at 500 hPa based on ERA-I and JRA-55), while at upper troposphere 5.2 g m⁻³ at 300 hPa MERRA. This explains the role of convection on the IWC amount in rainfall season. The concentration of IWC in the upper troposphere is explained by the liquid to ice conversion which has resulted in the

decrease in temperature with altitude in the troposphere. There are almost no IWC in the lower troposphere due to the temperature which has not yet reached the freezing point. As the cloud droplets are transported by winds in the higher altitudes, their temperature may reach the freezing point which leads to the ice clouds. The ERA-I and MERRA show the large average vertical IWC amount in East of Africa (4.1 and 6.5 g m⁻³, respectively) while JRA-55 shows it in South of Africa (3.75 g m⁻³). The highest amount of LWC is in East Africa due to large heating and convective systems which often develop cumulonimbus clouds and sometimes may result in lightning as it is close to the equator. South of Africa is a region located in midlatitude where there is winter season which may enhance the amount of IWC due to the significant drop in temperature from low to upper troposphere. The increase and the decrease of the liquid amount with temperature are predominantly due to the increase and decrease in LWP and IWP, respectively, with temperature (Shupe et al. 2006). These results based on ERA-I and MERRA confirm the ISCCP results in which the highest annual average amount of Cirrus (Ci) (ice cloud) is in East of Africa (18.4 %) (Fig. 5). We may say also that there is an agreement between JRA-55 and ISCCP due to highest annual average amount of Cirrus (Ci) in South of Africa (16.2 %) (Fig. 5). This is the evidence that the three reanalyses data are reliable and suitable for cloud studies. The low average vertical IWC amount is shown in North of Africa based on ERA-I (1.82 g m⁻³) and MERRA (3.3 g m⁻³) while JRA-55 shows it in East of Africa (1.05

g m^{-3}). This confirms the ISCCP results which show the lowest amount of Cirrus (Ci) in North of Africa (4.5 %) (Fig. 4). However, the JRA-55 shows the lowest IWC in East of Africa which disagrees with the ISCCP highest Cirrus amount in East of Africa. This may reveal some uncertainties to detect ice cloud with low amounts. The North of Africa is located in midlatitude region whereby during winter season the temperature drop enables the liquid-ice conversion leading to high amount of ice clouds. Among cloud type with ice, the Cirrus (Ci) clouds are the ones with high amount. This fact makes us to analyzed and compared them with ice clouds content (ICW) from the reanalyses data used in this paper. Cloud type distributions with liquid and ice contents in Africa are not the same (Fig. 4). We have related LWC and IWC vertical structure distribution given by ERA-interim to the cloud types given by ISCCP to know how they are distributed in different cloud types by region and season. The cloud types in the low troposphere have almost no ice. There are some differences of cloud type with liquid and ice content by season

in Africa, whereby cloud with high ice content occurred during MAM for 3 regions (East Africa, West Africa and North Africa) whereas during DJF in South Africa. The cloud with high amount in the low, mid and upper troposphere is Stratocumulus (Sc) (13.3 % in JJA), Altostratus (As) (10.7 % in MAM) and Cirrus (Ci) (24.6 % in MAM) in East of Africa, Stratocumulus (Sc) (19.3 % in SON), Altostratus (As) (9.4 % in JJA) and Cirrus (Ci) (20.4 % in MAM) in West of Africa, Cumulus (Cu) (8.67 % in MAM), Altostratus (As) (5.3 % in MAM) and Cirrus (Ci) (21.3 % in SON) in South of Africa and is Cumulus (Cu) (13.5 % in MAM), Altostratus (As) (10.3 % in SON) and Cirrus (Ci) (7.2 %) in North of Africa as shown in Fig. 4a–d, respectively. The maximum cloud fraction is located at the annual-mean position of the ITCZ near 5°C as shown by Mokhov (1994). The SAGE II showed 10–20 % in the tropics (Xaohan et al. 1995) which is in contrast to our results which show high cirrus amount. East and North Africa have more and less annually cloud amount, respectively (Fig. 4). The movement of ITCZ across East

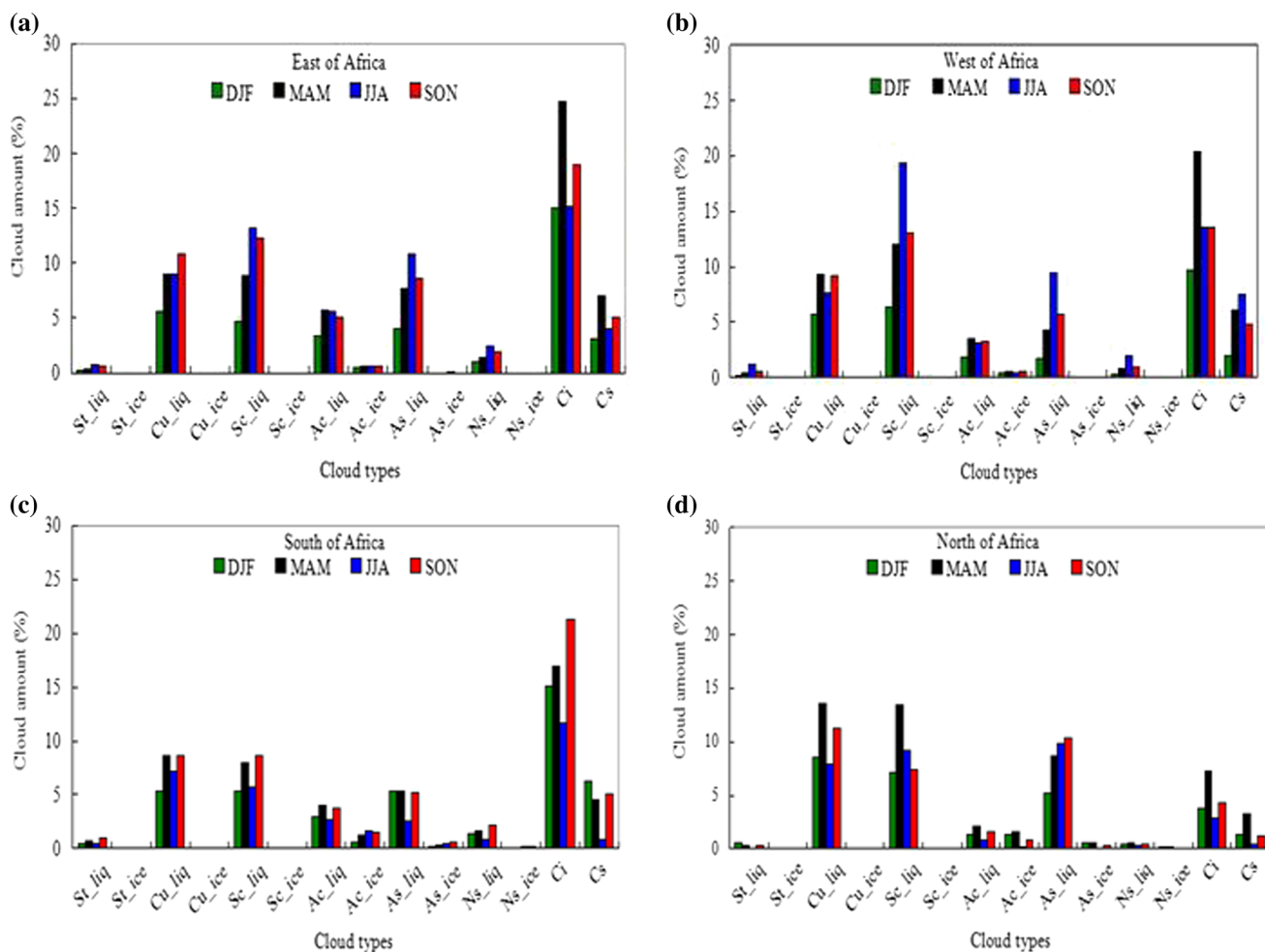


Fig. 4 Cloud amount seasonal average of cloud types with liquid and ice content in **a** East of Africa, **b** West of Africa, **c** South of Africa and **d** North of Africa based on ISCCP data from 1983 to 2009

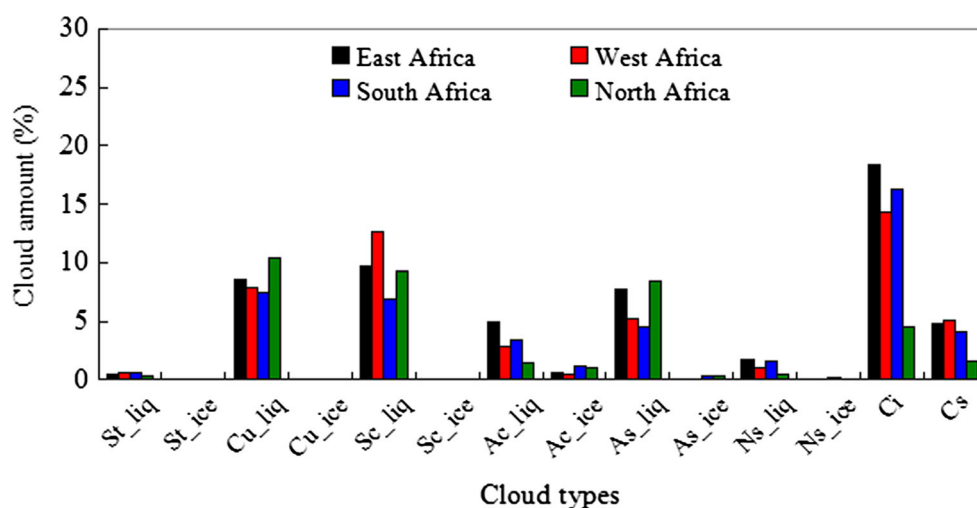


Fig. 5 Annual mean of cloud type amount with liquid and ice content in: **a** East of Africa, **b** West of Africa, **c** South of Africa and **d** North of Africa based on ISCCP data from 1983 to 2009

Africa two times annually explains high cloud amount in East Africa. The less cloud amount in North Africa is explained by less evaporation due to big area occupied by Sahara desert. Cloud amount in Africa shows a double peak in north and south of the equator while both the lower average amount and the double structure are associated with the seasonal variation in the intensity and position of ITCZ which is in agreement with our results which show high cloud amount in East Africa (Fig. 4). One of the regions with minimum cloud fraction includes Sahara and Kalahari deserts (Mokhov 1994). There is largest latitudinal contrast in cloud amounts in the tropics and subtropics and the vertical variation of the liquid fraction is cloud type dependent (Rossow et al. 1993). Ice clouds generally are extensive in the tropics for both land and ocean areas, where there are associated with deep convective clouds over land in the Congo basin (King et al. 2013). This explains the Fig. 4, which shows more cloud amount in East Africa (which covers both Northern and Southern hemisphere) and South Africa than West Africa and North Africa which are located in Northern hemisphere. In the previous study the relative humidity was found to be larger at the level where there are clouds and it is high in tropics and northern hemisphere than southern hemisphere (Inoue and Kamahori 2001). This explains the climatic features in tropics where East and West Africa are located and both North and South subtropics where South and North Africa are located. The analysis 219 of in situ measurements has shown that there is no correlation between IWC and LWC in mixed-phase clouds (Korolev et al. 2003). Previous studies have shown the variation of LWC and IWC with temperature but with different amount. In their studies Smith (1990), Moss and Johnson (1994) the LWC was found at $T < -15$ °C while Gultepe and Isaac (1997)

found that it between -30 and -25 °C. Hu et al. (2010) showed that 95 % of the liquid clouds can be found in the temperature range between -15 and 0 °C and the arctic mixed-phase cloud temperature ranges were found between -26 and -6 °C by Fukuta (1969). Cloud ice were observed also above 0 °C due to the fact that ice crystals melt when the wet bulb temperature exceeds 0 °C, while the UK Meteorological Office Unified Model assumed mixed phase clouds to exist between -15 and 0 °C (Gregory and Morris 1996). The liquid fraction as function of temperature was developed as scheme for parameterization in the UK Met Office atmospheric general circulation model and has assumed that all clouds are liquid at temperatures greater than 0 °C and ice lower than -15 °C as shown by Smith (1990). In this study the temperature (T) values correspond to pressure levels considered (from 1000 to 100 hPa). The coexistence temperature range between LWC and IWC in East of Africa (Fig. 6a–d), in West of Africa (Fig. 6e–h), in South of Africa (Fig. 6i–l), in North of Africa (Fig. 6m–p) during DJF, MAM, JJA and SON, respectively, based on ERA-I, JRA-55 and MERRA are explained in Table 3. We have calculated the annual mean from the seasonal mean (Table 3) to know the temperature range at which the mixed liquid and ice water clouds can be found: -22.7 °C $\leq T \leq 2.1$ °C, -16.4 °C $\leq T \leq 1.2$ °C, -54.3 °C $\leq T \leq 1.8$ °C in East of Africa, from -23.7 °C $\leq T \leq 2.1$ °C, -17.6 °C $\leq T \leq 0.7$ °C, -48.5 °C $\leq T \leq 1.6$ °C in West of Africa, 24.7 °C $\leq T \leq 5.5$ °C, -20.1 °C $\leq T \leq 4.7$ °C, -54.6 °C $\leq T \leq 3.4$ °C in South of Africa, from -23.3 °C $\leq T \leq 3.3$ °C, -20.9 °C $\leq T \leq 4.3$ °C, -33.2 °C $\leq T \leq 3.5$ °C in North of Africa based on ERA-I, JRA-55 and MERRA, respectively. The LWC and IWC coexistence temperature of ERA-I, JRA-55 and MERRA

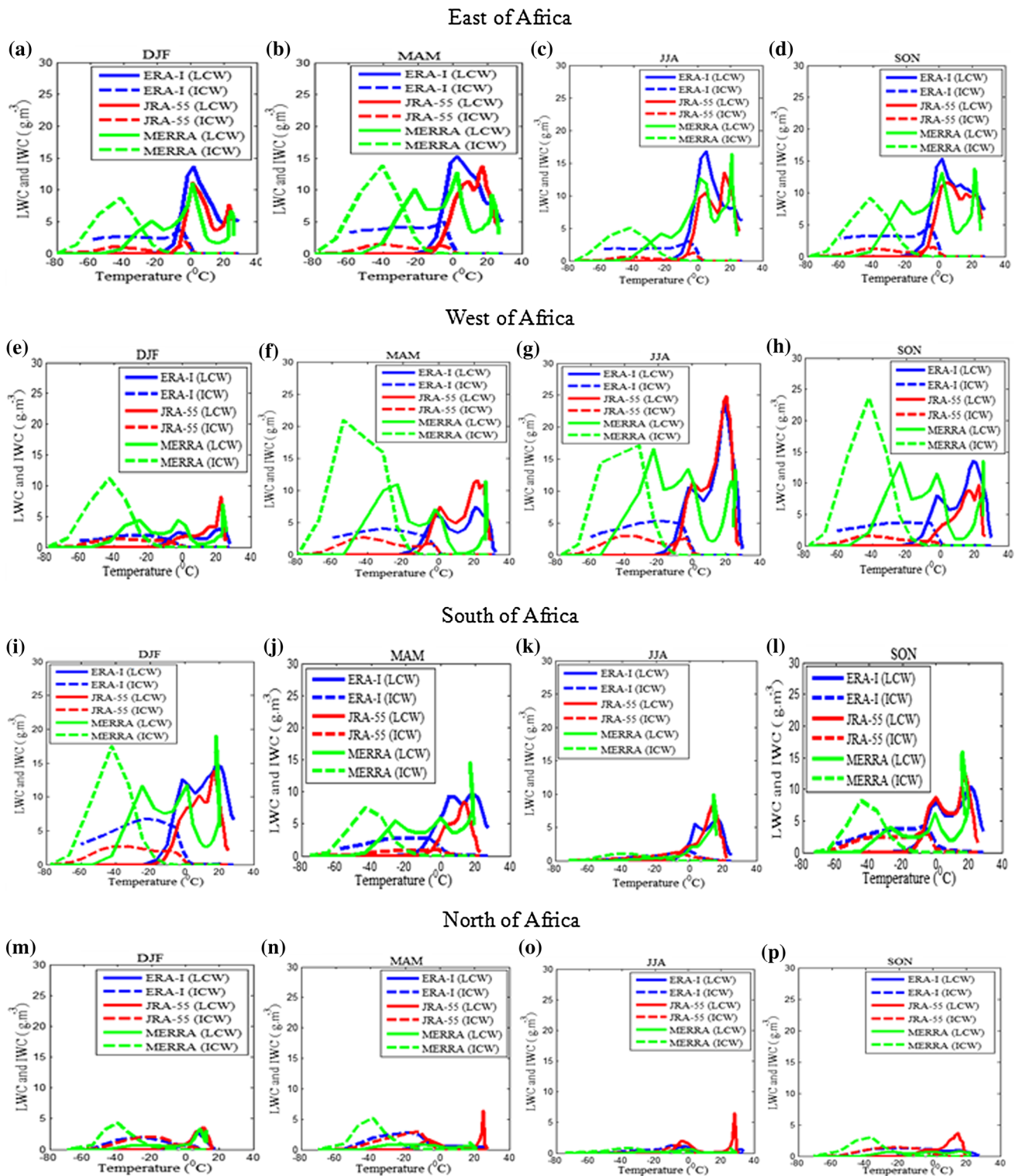


Fig. 6 The LWC (g m^{-3}) and IWC (g m^{-3}) seasonal variability with temperature (0°C) in East of Africa during **a** DJF, **b** MAM, **c** JJA, **d** SON; in West of Africa during **e** DJF, **f** MAM, **g** JJA, **h** SON; in South of Africa during **i** DJF, **j** MAM, **k** JJA, **l** SON and in North of

Africa during **m** DJF, **n** MAM, **o** JJA, **p** SON from ERA-I (blue line), JRA-55 (red line) and MERRA (green line) reanalysis from 1979 to 2014

are in good agreement at the temperatures above 0°C whereas only ERA-I and JRA-55 are in good agreement at the temperature below 0°C . The MERRA shows too low

temperatures in all regions of Africa which reveals its advantage to be used to detect the temperature at which exist the supercooled water liquid and ice clouds. The

Table 3 The coexistence temperature (T) interval between LWC and IWC in Africa by season based on ERA interim, JRA55 and MERRA reanalysis

Temperature	East of Africa	West of Africa	South of Africa	North of Africa
DJF				
ERA	$-22.9\text{ °C} \leq T \leq 2.1\text{ °C}$	$-24.9\text{ °C} \leq T \leq 1.6\text{ °C}$	$-22.9\text{ °C} \leq T \leq 2.3\text{ °C}$	$-25.6\text{ °C} \leq T \leq 4.9\text{ °C}$
JRA55	$-16.4\text{ °C} \leq T \leq 1.3\text{ °C}$	$-18.3\text{ °C} \leq T \leq 0.8\text{ °C}$	$-17.6\text{ °C} \leq T \leq 1.1\text{ °C}$	$-15.1\text{ °C} \leq T \leq 6.4\text{ °C}$
MERRA	$-54.7\text{ °C} \leq T \leq 1.7\text{ °C}$	$-53.7\text{ °C} \leq T \leq 1.8\text{ °C}$	$-54.9\text{ °C} \leq T \leq 1.4\text{ °C}$	$-40.1\text{ °C} \leq T \leq 2\text{ °C}$
MAM				
ERA	$-22.1\text{ °C} \leq T \leq 2.6\text{ °C}$	$-23.4\text{ °C} \leq T \leq 1.8\text{ °C}$	$-24.5\text{ °C} \leq T \leq 5\text{ °C}$	$-23.5\text{ °C} \leq T \leq 2.2\text{ °C}$
JRA55	$-16.2\text{ °C} \leq T \leq 1.5\text{ °C}$	$-17.4\text{ °C} \leq T \leq 0.8\text{ °C}$	$-20.7\text{ °C} \leq T \leq 5.1\text{ °C}$	$-23.9\text{ °C} \leq T \leq 7.2\text{ °C}$
MERRA	$-53.4\text{ °C} \leq T \leq 2.4\text{ °C}$	$-31.4\text{ °C} \leq T \leq 1.8\text{ °C}$	$-54.2\text{ °C} \leq T \leq 0.19\text{ °C}$	$-38.8\text{ °C} \leq T \leq -2.5\text{ °C}$
JJA				
ERA	$-23.1\text{ °C} \leq T \leq 2.1\text{ °C}$	$-22.9\text{ °C} \leq T \leq 1.8\text{ °C}$	$-26.1\text{ °C} \leq T \leq 5.7\text{ °C}$	$-22.9\text{ °C} \leq T \leq 2.8\text{ °C}$
JRA55	$-16.8\text{ °C} \leq T \leq 0.8\text{ °C}$	$-17.2\text{ °C} \leq T \leq 0.5\text{ °C}$	$-22.5\text{ °C} \leq T \leq 4.6\text{ °C}$	$-20.2\text{ °C} \leq T \leq 0.1\text{ °C}$
MERRA	$-54.9\text{ °C} \leq T \leq 1.5\text{ °C}$	$-54.2\text{ °C} \leq T \leq 1.5\text{ °C}$	$-54.4\text{ °C} \leq T \leq 4.3\text{ °C}$	$-17.3\text{ °C} \leq T \leq 2.5\text{ °C}$
SON				
ERA	$-22.8\text{ °C} \leq T \leq 1.8\text{ °C}$	$-23.8\text{ °C} \leq T \leq 1.4\text{ °C}$	$-25.4\text{ °C} \leq T \leq 9.3\text{ °C}$	$-21.2\text{ °C} \leq T \leq 3.4\text{ °C}$
JRA55	$-16.3\text{ °C} \leq T \leq 1.2\text{ °C}$	$-17.8\text{ °C} \leq T \leq 1\text{ °C}$	$-19.6\text{ °C} \leq T \leq 8\text{ °C}$	$-24.6\text{ °C} \leq T \leq 3.6\text{ °C}$
MERRA	$-54.3\text{ °C} \leq T \leq 1.6\text{ °C}$	$-54.7\text{ °C} \leq T \leq 1.4\text{ °C}$	$-54.9\text{ °C} \leq T \leq 7.8\text{ °C}$	$-36.7\text{ °C} \leq T \leq 7.1\text{ °C}$

amount of ice (liquid) water substance decreases (increases) with increasing temperature (Carey et al. 2008). The cloud water substance is in ice form at temperatures below -20 °C and the mass fraction of liquid (ice) water increases (decreases) linearly to unity (zero) as the temperature approaches 0 °C (Khairoutdinov and Randall 2003). In the global climate model the ice and liquid water content clouds parameterization must take consider the frequently distribution of all cloud types (ice, liquid water and mixed phase) as a function of temperature (Lin and Rossow 1996). The coexistence temperature variability in Africa influence the LWC and IWC amounts distributions. MERRA disagrees with both ERA-I and JRA-55 especially for negative temperatures while there are some agreements for positive temperatures. MERRA tends to overestimate and underestimate both ERA-I and JRA-55 for negative and positive temperature, respectively, in almost all regions over Africa (Fig. 6). The mixed-phase conditions show a transitory state as ice crystals will tend to grow at the expense of the liquid droplets, whereby with enough moisture supply and updraft speed, enough condensate can be produced for both deposition on ice and condensation on droplets to occur (Politovich 2003). The temperature $< -40\text{ °C}$ was detrained entirely as cloud ice by using the general circulation model (Fowler et al. 1996). In this study also we found MERRA with too low temperature in the upper troposphere in almost all regions of Africa. Liquid clouds were observed at temperature between -5 and -9 °C , ice crystal at temperature as warm as -14 °C and mixed phase clouds between -5 and -20 °C at height below 2 km, while all clouds between 2 and 5 km were

mixed-phase clouds (Pinto et al. 2001). There are 241 more water clouds in the lower troposphere, which are replaced by ice clouds in the upper troposphere following the temperature lapse rate (Fowler et al. 1996). In the previous studies the cloud liquid fraction in geographical regions between 72° N and 45° N showed no systematic dependence on latitude (Boudala et al. 2004), which is in contrast for this study where the LWC and IWC in East Africa and West Africa regions which are located in tropics regions show some differences in South of Africa and North of Africa which are located in both tropics and subtropics regions. Cloudiness minima are found in the subtropics ($20^\circ\text{--}25^\circ$) in each hemisphere, which reveals the descending branches of tropical Hadley and midlatitude Ferrel cell in each hemisphere (Mokhov 1994). The supercooled liquid water droplets may occur when the temperature of liquid water droplets fall into lower cold air temperature ($T < 0\text{ °C}$) (Politovich 2003). This may explain the presence of liquid in the coexistence temperature interval between liquid and ice shown in Table 3. The IWC occurs above the freezing level where the liquid water droplets are supercooled which explains the presence of IWC at upper pressure levels in all Africa during all seasons except in North and South of Africa where it occurs from mid to upper pressure levels. The liquid water droplets temperature fall at low-, middle- and upper pressure levels and there is formation of ice after reaching the freezing level during winter seasons in North and South of Africa. The soundings data were used to show the liquid, ice and mixed phase structure of different cloud types as a function of temperature (Mazin 2006). Our limitation is to

know the temperature interval at which cloud types may exist. Table 3 shows the coexistence temperature between LWC and IWC but also it reveals the temperature at which the supercooled water cloud may occur in all seasons in Africa. The reanalysis data cannot allow us to know at what negative temperature the supercooled water cloud occurs in every region of Africa by season due to the mixture of ice and supercooled water cloud droplets.

4 Conclusions

In this study, three recent reanalyses (ERA-I, JRA-55 and MERRA) have been used to evaluate the seasonal vertical profile of liquid and ice cloud content and their variability with temperature and to investigate the cloud type with low and high liquid/ice amounts based on ISCCP observations in East, West, South and North of Africa from climatology perspective. The important motivation for this study is to provide guidance regarding the distribution of liquid and ice water substance in cloud types for parameterizations in regional climate models. The three reanalysis and the ISCCP data products were used due to their long-period data availability of cloud types and both LWC and IWC, respectively. The three reanalyses are similar and consistent in describing the seasonal vertical profile over Africa. However, the differences among the reanalyses are clearly seen in the upper levels in over Africa. At the upper troposphere MERRA disagrees significantly with both ERA-I and JRA-55 in all seasons over Africa. There is remarkable agreement between ERA-I and JRA-55 in all regions and seasons in Africa from low to upper troposphere. The LWC and IWC based on MERRA are often high and low for negative and positive temperature, respectively, when compared to ERA-I and JRA-55. The three reanalyses show the maximum LWC in the lower or middle troposphere while the maximum IWC is found in the middle troposphere for both ERA-I and JRA-55, whereas in the upper troposphere for MERRA. The differences between both ERA-I and JRA-55 with MERRA become evident above 300 hPa. ERA-I and JRA-55 employ four-dimensional variational data assimilation (4DVAR) while MERRA uses three-dimensional variational data assimilation (3DVAR). This is one the reason which explains the significant consistency and agreement between ERA-I and JRA-55, while MERRA disagrees with both of them, especially at upper troposphere. Despite the vertical structure difference between MERRA with both ERA-I and JRA-55, there is no big difference in their LWC and IWC amount. The LWC is mostly concentrated in low and middle cloud levels while IWC in middle and high cloud levels and both LWC and IWC are dependent on temperature variability. The new findings in this study may help to

the understanding of cloud physics over Africa. The East and West Africa have more LWC and IWC than South and North Africa due to their latitude locations. The large and low average vertical LWC amount occurs in East and North of Africa due to the convective systems and less evaporation, respectively. The cloud type with highest liquid content is Stratocumulus (Sc) in both East and West of Africa while Cumulus (Cu) in both South and North of Africa. The Cirrus (Ci) clouds occur more frequently in Africa, where they occur during MAM in East, West and North of Africa. The vertical structure of LWC and IWC in the troposphere changes by season and by region, whereby the highest LWC and IWC occur during rainfall seasons. The LWC amount changes significantly whereas the IWC does not show significant variation in Africa by season and by region. The tropospheric range considered from 1000 and 100 hPa shows that the LWC and IWC may increase or decrease by altitude. At low troposphere the LWC increases by altitude while at middle- and high-pressure levels it decreases by altitude. The IWC increases from middle troposphere level and starts to increase by altitude from upper troposphere. We have analyzed the mentioned tropospheric range due to high LWC and IWC amounts. The difference in seasonal vertical distribution in Africa maybe explained by the differences in climatic features between tropical regions (East and West Africa) and subtropical regions (South and North Africa). The three reanalyses agree that the cloud liquid, supercooled cloud water and ice clouds occur between -22.7 and 1.6 °C over Africa. MERRRA tends to overestimate and underestimate both ERA-I and JRA-55 for negative and positive temperature, respectively, in almost all regions over Africa. The results obtained in this study are useful as they provide information on the seasonal vertical variability of LWC and IWC in different types of cloud in Africa from climatology perspective and may be used to evaluate LWC, IWC and temperature relationship while using climate models. The results show the differences in the LWC and IWC seasonal amount between East Africa, West Africa, South Africa and North of Africa. The results also reveal the cloud type with high liquid and ice content and their amount in Africa for each season. The benefit in using the corrected version of ISCCP from 1983 to 2009 in this study is its usefulness for regional cloud studies (Norris and Evan 2015) as we did for each region of Africa. Another benefit of using ISCCP observations and ERA-I, JRA-55, MERRA reanalysis are their abilities to provide long period cloud types and their liquid and ice contents, respectively, which allowed us to study the climatology of cloud types. The ISCCP long-term datasets are valuable for understanding cloud climatology trends (Carey et al. 2008). There are still no satellite or ground observation sensors which provide cloud types data of 26 years as ISCCP does. The limitation

of the corrected version of ISCCP from 1983 to 2009 is that it increases the cloud fraction in large part of North of Africa (Norris and Evan 2015) which may have influence on our results in that region. Another limitation is that we cannot know at what extent of negative temperature the supercooled water cloud occurs in every region of Africa by season due to the mixture of ice and supercooled water cloud droplets which occur below 0 °C. By comparing ISCCP and ERA-I, JRA-55, MERRA reanalysis we are limited to know the temperature interval at which cloud types may exist. In this study we relate the pressure levels of ISCCP cloud types and that of LWC and IWC based on ERA-I, JRA-55 and MERRA in order to assume the contents and LWC and IWC of each cloud types and the temperature interval for each cloud type. One of the issues is the low Nimbostratus amount in East of Africa during rainfall (MAM and SON), West of Africa (JJA), South of Africa (DJF) and North of Africa (DJF) which may be explained by the presence of upper clouds which may obscure the detection of low- and middle-level clouds as you mentioned. This shows that the ISCCP shows high amount of non-precipitating cloud during rainfall season in some regions which may have impacts on the way we relate it to the LWC and IWC amount of each cloud type. The ISCCP allows us to study cloud climatology but it relies only on two spectral channels while the most advanced satellite sensors offer over 20 spectral bands (Kotarba 2015). The Mount Pinatubo aerosols caused thin Cirrus clouds to be misidentified as low-level Cumulus clouds (Luo et al. 2002). The ISCCP may miss or be able to detect Cumulus clouds which leads to an underestimation or overestimation, respectively, of low cloud coverage (Rozendaal et al. 1995). Due to high dust aerosols in Sahara desert, the cirrus clouds may be misidentified as low-level Cumulus clouds. This may influence our results of Cirrus and Cumulus amount in North and West of Africa where Sahara desert is located. The high concentration of atmospheric aerosols shows a strong relationship with the position of ITCZ and monsoon rainfall over Africa (De Graaf et al. 2009). The rainfall due to convective systems is associated with the ITCZ migration (Maidment et al. 2014). The ISCCP was evaluated with MODIS and the results show that it has the ability to estimate correctly the cloud amount during warm season while it underestimates it during winter season in Central Europe (Kotarba 2015) which may also occur in Africa. Among the three reanalysis data used in this study, the ERA-I and JRA-55 are in good agreement from low to upper troposphere, which make us to suggest them to be used as proxies to monitor precipitation and cloud amounts in many regions with a lack of in situ observations in Africa. The caution should be taken when using reanalysis data products at regional scale for specific regions due to their obvious uncertainties.

The in situ observations instruments are needed in Africa and helpful for further research efforts in order to understand more about microphysics of clouds. The results presented in this study suggest that the reanalysis data products may allow us to improve the quality of regional climate model.

Acknowledgments The corresponding author appreciates the guidance, help and suggestions of his Supervisor Prof. Hongbin Chen and useful comments of reviewers. The authors thank Dr. Morgan Yarker for her time and constructive comments which helped to improve this paper. The authors would like also to thank ECWMF, Japanese Meteorological Agency and NASA for providing data used in this study. Authors also thank and appreciate the sponsorship provided by CAS-TWAS cooperation.

References

- Ackerman AS, Toon OB, Stevens DE, Heymsfield AJ, Ramanathan V, Welton EJ (2000) Reduction of tropical cloudiness by soot. *Science* 288:1042–1047. doi:10.1126/science.288.5468.1042
- Adeyewa ZD, Nakamura K (2003) Validation of TRMM radar rainfall data over major climatic regions in Africa. *J Appl Meteorol* 42:331–347. doi:10.1175/1520-0450(2003)042
- Albrecht B (1989) Aerosols, cloud microphysics, and fractional cloudiness. *Science* 245(1227–1230):1989
- Anyah RO, Semazzi FHM (2007) Variability of East African rainfall based on multiyear RegCM3 simulations. *Int J Climatol* 27:357–371
- Aufm KHJ (1950) Visibility and liquid water content in clouds in the free atmosphere. *J Meteorol* 7(54–57):1950. doi:10.1175/1520-0469007
- Bao X, Zhang F (2013) Evaluation of NCEP-CFSR, NCEP-NCAR, ERA-Interim, and ERA-40 reanalysis datasets against independent sounding observations over the Tibetan Plateau. *J Clim* 26:206–214. doi:10.1175/JCLI-D-12-00056.1
- Boucher O, Le Treut H, Baker MB (1995) Precipitation and radiation modeling in a general circulation model: Introduction of cloud microphysical processes. *J Geophys Res* 1995(100):16395–16414. doi:10.1029/95JD013
- Boudala SF, Isaac AG, Cober SG, Fu Q (2004) Liquid fraction in stratiform mixed-phase clouds from in situ observations. *Q J R Meteorol Soc* 130:2919–2931. doi:10.1256/qj.03.153
- Carey LD, Niu J, Yang P, Kankiewicz JA, Larson VE, Vonder Haar TH (2008) The vertical profile of liquid and ice water content in midlatitude mixed-phase altocumulus clouds. *J Appl Meteorol Climatol* 47:2487–2495. doi:10.1175/2008JAMC1885.1
- Chen G, Iwasaki T, Qin H, Sha W (2014) Evaluation of the warm-season diurnal variability over East Asia in recent reanalyses JRA-55, ERA-Interim, NCEP CFSR, and NASA MERRA. *J Clim* 27(5517–5537):2014
- Cooke W, Koffi B, Grégoire JM (1996) Seasonality of vegetation fires in Africa from remote sensing data and application to a global chemistry model. *J Geophys Res* 101(D15):21051–21065. doi:10.1029/96JD01835
- Dee DP, Uppala SM, Simmons AJ, Berrisford P, Poli P, Kobayashi S, Andrae U, Balmaseda MA, Balsamo G, Bauer P, Bechtold P, Beljaars ACM, Van de Berg L, Bidlot J, Bormann N, Delsol C, Dragani R, Fuentes M, Geer AJ, Haimberger L, Healy SB, Hersbach H, Holm EV, Isaksen L, Kallberg P, Kohler M, Matricardi M, McNally AP, Monge-Sanz BM, Morcrette JJ, Park BK, Peubey C, De Rosnay P, Tavolato C, Thépaut J-N, Vitart F (2011) The ERA-Interim reanalysis: configuration and

- performance of the data assimilation system. *Q J R Meteorol Soc* 137:553–597
- De Graaf M, Tilstra LG, Aben I, Stammes P (2009) Satellite observations of the seasonal cycles of absorbing aerosols in Africa related to the monsoon rainfall, 1995–2008. *Atmos Environ* 44:1274–1283. doi:[10.1016/j.atmosenv.2009.12.038](https://doi.org/10.1016/j.atmosenv.2009.12.038)
- DelGenio AD, Wolf AB (2000) The temperature dependence of the liquid water path of low clouds in the southern great plains. *J Clim* 2000(13):3465–3486
- Engelbrecht CJ, Landman WA (2015) Interannual variability of seasonal rainfall over the Cape south coast of South Africa and synoptic type association. *Clim Dyn*. doi:[10.1007/s00382-015-2836-2](https://doi.org/10.1007/s00382-015-2836-2)
- Fabien S, Mallet M, Elguindi N, Giorgi F, Zakey A, Konaré A (2008) Dust aerosol impact on regional precipitation over western Africa, mechanisms and sensitivity to absorption properties. *J Geophys Res* 113:L24705. doi:[10.1029/2008GL035900](https://doi.org/10.1029/2008GL035900)
- Fowler LD, Randall DA, Rutledge SA (1996) Liquid and ice microphysics in the CSU general circulation model. Part I: Model description and simulated microphysical processes. *J Clim* 1996(9):489–529
- Fukuta N (1969) Experimental studies of the growth of small ice crystal. *L Atmos Sci* 1969(26):522–531
- Geerts B, Dejene T (2005) Regional and diurnal variability of the vertical structure of precipitation systems in Africa based on spaceborne Radar data. *J Clim* 18:893–916. doi:[10.1175/JCLI-3316.1](https://doi.org/10.1175/JCLI-3316.1)
- Gregory D, Morris D (1996) The sensitivity of climate simulations to the specifications of mixed phase clouds. *Clim Dyn* 12(9):641–651
- Gu Y, Liou KN, Jiang JH, Su H, Liu X (2012) Dust aerosol impact on North Africa climate: a GCM investigation of aerosol-cloud-radiation interactions using A-Train satellite data. *Atmos Chem Phys*. doi:[10.5194/acp-12-1667-2012](https://doi.org/10.5194/acp-12-1667-2012)
- Gultepe I, Isaac A (1997) Liquid water content and temperature relationship from aircraft observations and its applicability to GCMs. *J Clim* 1997(10):446–452
- Gultepe I, Isaac GA, Cober SG (2002) Cloud microphysical characteristics versus temperature for three Canadian field projects. *Ann Geophys Eur Geosci Union (EGU)* 20(11):1891–1898
- Harrington JY, Reisen T, Cotton WR, Kreidenweis SM (1999) Cloud resolving simulations of Arctic stratus. Part II: transition-season clouds. *Atmos Res* 1999(51):45–75
- Hodges KI, Lee RW, Bengtsson L (2011) A comparison of extratropical cyclones in recent reanalyses ERA-Interim, NASA MERRA, NCEP CFSR, and JRA-25. *J Clim* 24:4888–4906
- Houze AHJ (1997) Stratiform precipitation in regions of convection: a meteorological paradox? *Bull Am Meteorol Soc* 78:2179–2196. doi:[10.1175/1520-0477078](https://doi.org/10.1175/1520-0477078)
- Hu Y, Rodier S, Xu K, Sun W, Huang J, Lin B, Zhai P, Josset D (2010) Occurrence, liquid water content, and fraction of supercooled water clouds from combined CALIOP/IIR/MODIS measurements. *J Geophys Res* 115:D00H34. doi:[10.1029/2009JD012384](https://doi.org/10.1029/2009JD012384)
- Huffman GJ, Adler RF, Arkin P, Chang A, Ferraro R, Gruber A, Janowiak J, McNab A, Rudolf B, Schneider U (1997) The global precipitation climatology project (GPCP) combined precipitation dataset. *Bull Am Meteorol Soc* 78:5–20
- Inoue T, Kamahori H (2001) Statistical relationship between ISCCP cloud type and vertical relative humidity profile. *J Meteorol Soc Jpn* 79(6):1243–1256
- Janicot S, Sultan B (2001) Intra-seasonal modulation of convection in the West African Monsoon. *J Geophys Res*. doi:[10.1029/2000GL012424](https://doi.org/10.1029/2000GL012424)
- Jiang X, Waliser DE, Li JL (2011) Vertical cloud structures of the boreal summer intraseasonal variability based on CloudSat observations and ERA-interim. *Clim Dyn* 2011(36):2219–2232. doi:[10.1007/s00382-010-0853-8](https://doi.org/10.1007/s00382-010-0853-8)
- Kennedy AD, Dong X, Xi B, Xie S, Zhang Y, Chen J (2011) A comparison of MERRA and NARR reanalyses with the DOE ARM SGP data. *J Clim* 24:4541–4557. doi:[10.1175/2011JCLI3978.1](https://doi.org/10.1175/2011JCLI3978.1)
- Khairoutdinov MF, Randall DA (2003) Cloud resolving modeling of the ARM summer 1997 IOP: model formulation, results, uncertainties, and sensitivities. *J Atmos Sci* 60(607–625):2003
- Kiladis GN, Weickmann KM (1997) Horizontal structure and seasonality of large-scale circulations associated with sub-monthly tropical convection. *Mon. Wea. Rev.* 125:1997–2013
- King MD, Platnick S, Menzel WP, Ackerman SA, Hubanks PA (2013) Spatial and temporal distribution of clouds observed by MODIS onboard the Terra and Aqua satellites. *IEEE Trans Geosci Remote Sens* 51:7
- Kobayashi S, Ota Y, Harada Y, Ebata A, Moriya M, Onoda H, Onogi K, Kamahori H, Kobayashi C, Endo H, Miyaoka K, Takahashi K (2015) The JRA-55 reanalysis: general specifications and basic characteristics. *J Meteorol Soc Jpn* 93:5–48. doi:[10.2151/jmsj.2015-001](https://doi.org/10.2151/jmsj.2015-001)
- Korolev AV, Isaac G (2003) Phase transformation of mixed-phase clouds. *Q J Roy Meteorol Soc* 129:19–38. doi:[10.1256/qj.203](https://doi.org/10.1256/qj.203)
- Korolev AV, Isaac GA, Cober SG, Walter SJ, Hallett J (2003) Microphysical characterization of mixed-phase clouds. *Q J R Meteorol Soc* 129:39–65. doi:[10.1256/qj.01.204](https://doi.org/10.1256/qj.01.204)
- Kotarba AZ (2015) Evaluation of ISCCP cloud amount with MODIS observations. *Atmos Res* 153(310–317):2015
- Lin B, Rossow WB (1996) Seasonal variation of liquid and ice water path in no precipitating clouds over oceans. *J Clim* 9(2890–2902):1996
- Lindsay R, Wensnahan M, Schweiger A, Zhang J (2014) Evaluation of seven different atmospheric reanalysis products in the arctic. *J Clim* 27:2588–2606
- Luo Z, Rossow WB, Inoue T, Stubenrauch CJ (2002) Did the eruption of the Mt. Pinatubo volcano affect cirrus properties? *J Clim* 15:2806–2820
- Mahowald NM, Kiehl LM (2003) Mineral aerosol and cloud interactions. *J Geophys Res* 30(9):1475
- Maidment RI, Grimes D, Allan RP, Tamnasky E, Stringer M, Hewison Tim, Roebeling R, Black E (2014) The 30 year TAMSAT African rainfall climatology and time series (TAR-CAT) data set. *J Geophys*. doi:[10.1002/2014JD021927](https://doi.org/10.1002/2014JD021927)
- Mazin IP (2006) Cloud phase structure: experimental data analysis and parameterization. *J Atmos Sci* 2006(63):667–681
- Mike D (2002) Late Victorian Holocausts: El Niño famines and the making of the Third World. Verso, pp 263–266
- Mokhov II (1994) Analysis of global cloudiness 2. Comparison of ground-based and satellite-based cloud climatologies. *J Geophys Res* 99(D8):17045–17065
- Moller D, Acker K, Wierprecht W (1996) A relationship between liquid water content and chemical composition in clouds. *Atmos Res* 41:321–335. doi:[10.1016/0169-8095\(96\)00017-8](https://doi.org/10.1016/0169-8095(96)00017-8)
- Moreno SF, Mannaerts CM, Jetten V (2014) Influence of topography on rainfall variability in Santiago Island, Cape Verde. *Int J Climatol* 34:1081–1097
- Moss SJ, Johnson DW (1994) Aircraft measurements to validate and improve numerical model parameterizations of ice to water ratios in clouds. *Atmos Res* 1994(34):1–25
- Nikulin G, Jones C, Giorgi F, Asrar G, Büchner M, Ruth CM, Christensen OB, Déqué M, Fernandez J, Hänsler A, Erik VM, Samuelsson P, Sylla MB, Sushama L (2012) Precipitation climatology in an ensemble of CORDEX-Africa regional climate

- simulations. *J Clim* 25:6057–6078. doi:[10.1175/JCLI-D-11-00375.1](https://doi.org/10.1175/JCLI-D-11-00375.1)
- Noh YJ, Seaman CJ, Vonder Haar TH, Liu G (2013) In Situ Aircraft measurements of the vertical distribution of liquid and ice water content in midlatitude mixed-phase clouds. *J Appl Meteorol Climatol* 2013(52):269–279
- Norris JR, Evan AT (2015) Empirical removal of artifacts from the ISCCP and PATMOS-x satellite cloud records. *J Atmos Oceanic Technol* 32:691–702
- Ntale HK, Gan TY, Mwale D (2003) Prediction of East African Seasonal rainfall using simplex canonical correlation analysis. *J Clim* 16:2105–2112. doi:[10.1175/1520-0442\(2003\)016<2105:POEASR>2.0.CO;2](https://doi.org/10.1175/1520-0442(2003)016<2105:POEASR>2.0.CO;2)
- Ntwali D (2015) Comparison of spatial and temporal cloud coverage derived from CloudSat, CERES, ISCCP and their relationship with precipitation over Africa. *Am J Remote Sens* 3(2):17–28. doi:[10.11648/j.ajrs.20150302.11](https://doi.org/10.11648/j.ajrs.20150302.11)
- Ogallal LJ (1989) The spatial and temporal patterns of East African rainfall derived from principal component analysis. *Int J Climatol* 9:145–167
- Okoola ER (1999) A diagnostic study of the Eastern Africa Monsoon circulation during the Northern Hemisphere spring season. *Int J Climatol* 19:143–168
- Pawson S, Stajner I, Kawa SR, Hayashi H, Tan WW, Nielsen JE, Zhu Z, Chang LL, Livesey NJ (2007) Stratospheric transport using 6-h-averaged winds from a data assimilation system. *J Geophys Res* 112:D23103. doi:[10.1029/2006JD007673](https://doi.org/10.1029/2006JD007673)
- Pincus R, Baker MB (1994) Effect of precipitation on the albedo susceptibility of clouds in the marine boundary layer. *Nature* 372:250–252. doi:[10.1038/372250a0](https://doi.org/10.1038/372250a0)
- Pinto JO, Curry JA, Curry JA (2001) Cloud-aerosol interactions during autumn over Beaufort Sea. *J Geophys Res* 106(D14):15077–15097
- Politovich MK (2003) Aircraft icing. *Aviat Meteorol*. doi:[10.1016/B978-0-12-382225-3.00055-4](https://doi.org/10.1016/B978-0-12-382225-3.00055-4)
- Riehl H (1979) *Climate and Weather in the tropics*. Academic Press, Amsterdam, p 611
- Rienecker MM, Suarez MJ, Gelaro R, Todling R, Bacmeister J, Liu E, Bosilovich Michael G, Schubert Siegfried D, Takacs Lawrence, Kim GK, Bloom S, Chen J, Collins D, Conaty A, Arlindo DS, Gu W, Joiner J, Koster RD, Lucchesi R, Molod A, Owens T, Pawson S, Pegion P, Redder CR, Reichle R, Robertson FR, Ruddick AG, Sienkiewicz M, Woollen J (2011) MERRA: NASA's Modern-Era retrospective analysis for research and applications. *J Clim* 24:3624–3648
- Rosenfeld D (2000) Suppression of rain and snow by Urban and industrial air pollution. *Science* 2000(287):1793–1796
- Rosenfeld D, Rudich Y, Lahav R (2001) Desert dust suppressing precipitation: a possible desertification feedback loop. *Proc Natl Acad Sci USA*. doi:[10.1073/pnas.101122798](https://doi.org/10.1073/pnas.101122798)
- Rossow WB, Schiffer RA (1991) ISCCP cloud data products. *Bull Am Meteorol Soc* 1991(71):2–20
- Rossow WB, Walker AW, Gardner LC (1993) Comparison of ISCCP and other cloud amounts. *J Clim* 6(12):2394–2418
- Rui L, Yunfei F (2005) Tropical precipitation by GPCP and TRMM PR observations. *Adv Atmos Sci* 22(6):852–864
- Rutledge SA, Houze RA Jr (1987) A diagnostic modelling study of the trailing stratiform region of a midlatitude squall line. *J Atmos Sci* 44:2640–2656
- Sakaeda N, Wood R, Rasch PJ (2011) Direct and semidirect aerosol effects of southern African biomass burning aerosol. *J Geophys Res* 116:D12205. doi:[10.1029/2010JD015540](https://doi.org/10.1029/2010JD015540)
- Shupe MD, Matrosov SY, Uttal T (2006) Arctic mixed-phase cloud properties derived from surface-based sensors at SHEBA. *J Atmos Sci* 63:697–711
- Smith RNB (1990) A scheme for predicting layer clouds and their water content in a general circulation model. *Q J Roy Meteorol Soc* 1990(116):435–460
- Stein DC, Swap RJ, Greco S, Piketh SJ, Macko SA, Doddridge BG, Elias T, Brintjes RT (2003) Haze layer characterization and associated meteorological controls along the eastern coastal region of southern Africa. *J Geophys Res* 108:D13. doi:[10.1029/2002JD003237](https://doi.org/10.1029/2002JD003237)
- Tierney JE, Lewis SC, Cook BI, LeGrande AN, Schmidt GA (2011) Model, proxy and isotopic perspectives on the East African humid period. *Earth Planet Sci Lett*. doi:[10.1016/j.epsl.2011.04.038](https://doi.org/10.1016/j.epsl.2011.04.038)
- Tozuka T, Abiodun BJ, Engelbrecht FA (2014) Impacts of convection schemes on simulating tropical-temperate troughs over southern Africa. *Clim Dyn* 42:433–451
- Twomey SA (1977) The influence of pollution on the shortwave albedo of clouds. *J Atmos Sci* 34:1149–1152
- Twomey S, Gall R, Leuthold M (1987) Pollution and cloud reflectance. *Boundary Layer Meteorol* 41(1–4):335–348
- Uppala SM, Kållberg PW, Simmons AJ, Andrae U, Da Costa BVB, Fiorino M, Gibson JK, Haseler J, Hernandez A, Kelly GA, Li X, Onogi K, Saarinen S, Sokka N, Allan RP, Andersson E, Arpe K, Balmaseda MA, Beljaars ACM, Van De Berg L, Bidlot J, Bormann N, Caires S, Chevallier F, Dethof A, Dragosavac M, Fisher M, Fuentes M, Hagemann S, Hólm E, Hoskins BJ, Isaksen I, Janssen PAEM, Jenne R, McNally AP, Mahfouf JF, Morcrette JJ, Rayner NA, Saunders RW, Simon P, Sterl A, Trenberth KE, Untch A, Vasiljevic D, Viterbo P, Woollen J (2005) The ERA-40 re-analysis. *Q J Roy Meteorol Soc* 131:2961–3012
- Vidaurre G, Hallett J, Rogers DC (2011) Airborne measurement of liquid and total water content. *J Atmos Oceanic Technol* 2011(28):1088–1103
- Weisse AK, Bois P (2001) Topographic effects on statistical characteristics of heavy rainfall and mapping in French Alps. *J Appl Meteorol* 40:720–740
- Wu WS, Purser RJ, Parrish DF (2002) Three-dimensional variational analysis with spatially inhomogeneous covariances. *Monthly Weather Rev* 130:2905–2916
- Xaohan L, Ring D, Rossow WB (1995) Comparison between SAGE II and ISCCP high-level clouds, Part I: global and zonal mean cloud amounts. *J Geophys Res* 100:1121–1135
- Allan RJ (2000) ENSO and climatic variability in the last 150 years, in El Niño and the Southern Oscillation: multiscale variability, global and regional impacts. In: Diaz HF, Markgraf V (eds). Cambridge University Press, Cambridge, pp 3–56
- Yamada Y, Satoh M (2013) Response of ice and liquid water paths of tropical cyclones to global warming simulated by a global nonhydrostatic model with explicit cloud microphysics. *J Clim* 2013(26):9931–9945. doi:[10.1175/JCLI-D-13-00182.1](https://doi.org/10.1175/JCLI-D-13-00182.1)
- Yokoi S (2015) Multireanalysis comparison of variability in column water vapor and its analysis increment associated with the Madden–Julian oscillation. *J Clim* 28(793–808):2015. doi:[10.1175/JCLI-D-14-00465.1](https://doi.org/10.1175/JCLI-D-14-00465.1)
- Yoshioka M, Mahowald NM, Conley AJ, Collins WD, Fillmore DW, Zender CS, Coleman DB (2007) Impact of desert dust radiative forcing on Sahel precipitation: relative importance of dust compared to sea surface temperature variations, vegetation changes, and greenhouse gas warming. *J Clim* 20:1445–1467
- Zhang D, Wang Z, Liu D (2010) A global view of midlevel liquid-layer topped stratiform cloud distribution and phase partition from CALIPSO and CloudSat measurements. *J Geophys Res* 115:D00H13. doi:[10.1029/2009JD01214](https://doi.org/10.1029/2009JD01214)